



OPEN ACCESS

EDITED BY

Eva Krasakopoulou,
University of the Aegean, Greece

REVIEWED BY

Christoph Voelker,
Alfred Wegener Institute Helmholtz Centre
for Polar and Marine Research (AWI),
Germany
Alexandra Gogou,
Hellenic Centre for Marine Research
(HCMR), Greece

*CORRESPONDENCE

Anouk P. E. van Boxtel

✉ anouk.van.boxtel@nioz.nl

RECEIVED 29 November 2024

ACCEPTED 14 February 2025

PUBLISHED 05 March 2025

CITATION

van Boxtel APE, Stuut J-BW and Peterse F
(2025) Identifying Saharan dust driven export
of biogenic material in the ultraoligotrophic
eastern Mediterranean Sea.

Front. Mar. Sci. 12:1537028.

doi: 10.3389/fmars.2025.1537028

COPYRIGHT

© 2025 van Boxtel, Stuut and Peterse. This is
an open-access article distributed under the
terms of the [Creative Commons Attribution
License \(CC BY\)](https://creativecommons.org/licenses/by/4.0/). The use, distribution or
reproduction in other forums is permitted,
provided the original author(s) and the
copyright owner(s) are credited and that the
original publication in this journal is cited, in
accordance with accepted academic
practice. No use, distribution or reproduction
is permitted which does not comply with
these terms.

Identifying Saharan dust driven export of biogenic material in the ultraoligotrophic eastern Mediterranean Sea

Anouk P. E. van Boxtel^{1,2*}, Jan-Berend W. Stuut^{1,3}
and Francien Peterse²

¹Department of Ocean Systems, NIOZ Royal Netherlands Institute for Sea Research, Texel, Netherlands, ²Department of Earth Sciences, Utrecht University, Utrecht, Netherlands,

³Department of Earth Sciences, Vrije Universiteit Amsterdam, Amsterdam, Netherlands

To assess the effects of dust deposition on the strength of the biological pump in the Mediterranean Sea by acting as fertilizer and/or ballasting agent, we analyzed fluxes of mineral dust, particulate organic carbon (POC) and inorganic carbon (PIC), and source-specific lipid biomarkers (i.e., higher plant-derived long-chain fatty acids and phytoplankton-derived alkenones, C₃₀ 1,15 diols, and sterols) in sinking particles. Sinking particles were collected at ten-day intervals by a sediment-trap mooring deployed in the Ionian Basin from April 2017 to May 2018 at 2340 m water depth. High POC fluxes occur during summer, when surface ocean primary production is lowest due to thermal stratification. Notably, these high POC fluxes coincide with pulses of substantial dust deposition, suggesting that POC export is primarily driven by dust deposition and subsequent ballasting. However, the lipid composition, and thereby that of the phytoplankton community, differs between dust events. (Seasonal) variations in the properties of the deposited dust, presumably associated with its provenance, likely control the effect of dust deposition on phytoplankton response and export in the Ionian Basin. Although POC export is associated with dust deposition, the net effect of dust deposition on the biological pump is more ambiguous as not all dust events are associated with an increase in POC export, and most dust events are also associated with PIC export that has a counteracting effect on the biological pump. Multi-year time series of dust deposition and biogenic export are required to validate the seasonal variations in dust-driven export of biogenic material observed here, and to account for effects of interannual variations in dust fluxes and phytoplankton production on the strength of the biological pump.

KEYWORDS

dust fertilization, ballasting, carbon, biological pump, eastern Mediterranean Sea, lipid biomarkers, phytoplankton

1 Introduction

Deposition of atmospheric desert dust provides nutrients to remote oligotrophic areas of the world's ocean, thereby temporarily relieving nutrient limitation and stimulating primary production and associated carbon fixation (e.g., [Guerreiro et al., 2017](#); [Pabortsava et al., 2017](#); [Guerreiro et al., 2021](#)). If this fixed carbon is subsequently exported to the deep ocean, dust fertilization can in theory substantially contribute to carbon sequestration, given that oligotrophic regions comprise 60% of the global ocean surface ([Antoine et al., 1996](#)). One area where dust fertilization might play an important role in driving primary production is the eastern Mediterranean Sea (EMS) ([Ridame and Guieu, 2002](#); [Pulido-Villena et al., 2010](#); [Ridame et al., 2014](#)). The EMS is an ultraoligotrophic basin due to its anti-estuarine circulation resulting in a net loss of nutrients ([Krom et al., 2004](#)). Consequently, primary production is low, particularly in the eastern part of the basin. Dust transport to the EMS mainly occurs in spring – early summer and is a major source of new nitrogen and phosphate for the EMS ([Guerzoni et al., 1999](#); [Herut et al., 1999](#); [Guieu, 2002](#)), contributing ~60% and ~30% of the total nitrogen and phosphate supply, respectively ([Krom et al., 2004](#)). Several micro- and mesocosm experiments in the Mediterranean Sea have shown that Chl a concentrations and primary production rates increase after dust addition ([Herut et al., 2005](#); [Ridame et al., 2014](#); [Herut et al., 2016](#); [Gazeau et al., 2021b](#)), suggesting that dust input may indeed have a fertilizing effect. Additionally, dust addition stimulated substantial N $_2$ fixation by diazotrophs in a mesocosm experiment using water from the EMS, indirectly contributing to increased nitrogen availability ([Ridame et al., 2022](#)).

However, rather than stimulating the biological pump by serving as a fertilizer, dust deposition can also lead to a decrease in the strength of the biological pump. Instead of stimulating primary production, dust addition can also stimulate heterotrophic bacterial growth and remineralization of dissolved organic carbon (DOC) ([Herut et al., 2005](#); [Pulido-Villena et al., 2008](#); [Guieu et al., 2014](#); [Gazeau et al., 2021a](#)). Furthermore, dust deposition can also decrease carbon sequestration through increasing the strength of the carbonate counter pump, when particulate inorganic carbon (PIC) is exported instead of particulate organic carbon (POC): when calcifying phytoplankton precipitates CaCO $_3$ for their exoskeletons, CO $_2$ is also released. Hence, when CaCO $_3$ -producing phytoplankton, such as coccolithophores, benefit most from dust fertilization, the amount of CO $_2$ that is sequestered through fertilization is reduced. As calcifying coccolithophores are important primary producers in the Mediterranean Sea, in particular the opportunistic *Gephyrocapsa huxleyi* (formerly *Emiliania huxleyi*) ([Ignatiades et al., 2009](#); [Siokou-Frangou et al., 2010](#)), dust fertilization could lead to CO $_2$ release if mainly calcifying phytoplankton is stimulated.

Besides fertilizing effects, dust can affect the amount of carbon export through ballasting ([Armstrong et al., 2002](#)), where the deposition of relatively large and dense dust particles as well as (dust-induced) aggregate formation could stimulate the biological pump ([Ternon et al., 2010](#); [Bressac et al., 2014](#); [Louis et al., 2017](#);

[Van Der Jagt et al., 2018](#); [Guerreiro et al., 2019](#)), specifically in seasons with low zooplankton abundance ([Lee et al., 2009b](#)). Moreover, the ballasting capacity of dust is linked to its fertilizing effect on the phytoplankton community composition: incubation experiments have shown that repeated dust addition can change the composition of the phytoplankton community, switching from the naturally occurring picophytoplankton-dominated community to a nano- and micro phytoplankton-dominated community ([Giovagnetti et al., 2013](#); [Gazeau et al., 2021a](#)). As larger plankton sinks faster and mineral skeletons of specific phytoplankton groups provide extra material for ballasting, such a community shift can thus lead to a change in the strength of the biological pump.

Finally, also the properties and deposition mode of the dust that is deposited in the EMS play a role in its effect on the biological pump. For instance, the main sources and transport routes of the dust vary through the year ([Israelevich et al., 2012](#)). As different dust sources are likely to have different characteristics, such as nutrient content and bioavailability of nutrients, the exact effect of dust deposition on phytoplankton growth is likely to differ between dust events. Similarly, wet deposition, i.e., dust deposition along with precipitation, is considered to have a stronger fertilizing effect than dry deposition as nutrients in wet-deposited dust are more bioavailable due to pre-leaching of dust particles in acidic cloud conditions ([Ridame and Guieu, 2002](#); [Ridame et al., 2014](#); [Louis et al., 2018](#)).

Due to the various stimulating and inhibiting effects of dust on the biological pump, either through fertilization or through ballasting, and seasonal variation in oceanographic background conditions and dust transport, the net effect of dust deposition on carbon export in the Mediterranean Sea remains unclear and difficult to quantify. To assess these relationships, we here studied a continuous time series of sinking particles collected at a ten-day resolution by a sediment trap mooring deployed in the Ionian Basin from April 2017 to May 2018 at 2340 m water depth. To identify and quantify the relationships between Saharan dust deposition and export of biogenic material, fluxes of POC and PIC were compared to lithogenic fluxes, i.e., mineral dust, from the sediment-trap time series. Furthermore, to assess changes in the source of the exported marine biogenic material and the response of different phytoplankton groups to dust deposition, records of lipid biomarkers for specific phytoplankton groups (i.e., di- and tri-unsaturated long-chain alkenones, dinosterol, brassicasterol, and long chain C $_{30}$ 1,15 diols) were studied, complemented with cholesterol as a generic marker for organic material derived from higher trophic levels (zooplankton and fecal pellets). To gain insight into temporal variation in characteristics of the deposited dust, resembling variation in e.g., dust provenance, grain-size distributions of the lithogenic fraction and lipid biomarkers for terrestrial vegetation (long-chain fatty acids; LCFAs) were studied. Additionally, the sediment-trap records of sinking dust and marine biogenic particles were compared to remote-sensing time series of Chl a to connect particle export in the deep Mediterranean Sea to surface ocean productivity, to time series of precipitation rate to assess variation in deposition mode, and to time series of aerosol optical depth (AOD) to connect sediment-trap dust events to atmospheric dust events.

2 Material and methods

2.1 Oceanography of the study site

Large-scale circulation in the Ionian Sea consists of the inflow of modified Atlantic Water (MAW) at the surface that enters the Ionian Sea through the Sicily Channel and the outflow of Levantine Intermediate Water (LIW), that flows westward from the Levantine Basin at intermediate water depths (Poulos, 2023). Similar to the anti-estuarine circulation of whole Mediterranean Sea, this anti-estuarine circulation results in a loss of nutrients from the EMS to the WMS and a west-east decrease in primary productivity (Siokou-Frangou et al., 2010).

The main features of the EMS surface circulation consist of the MAW jet and several permanent or semi-permanent gyres, including the northern Ionian Gyre. The large-scale surface circulation in the EMS and main pathways of MAW and LIW are affected to a great extent by decadal variability in the direction of basin-scale circulation of the Ionian Sea. This reversal in surface circulation is the result of the Bimodal Oscillating System (BiOS), a feedback mechanism between Ionian Sea circulation inversions and the redistribution of water masses in the EMS (Gačić et al., 2010; Civitarese et al., 2023). These decadal reversals in the direction of surface circulation affect nutrient concentrations, primary production and phytoplankton phenology in the basin (Civitarese et al., 2010; Lavigne et al., 2018; Civitarese et al., 2023). Additionally, mesoscale features superimposed on these larger circulation patterns, such as mesoscale eddies, result in spatial heterogeneity in nutrient concentrations and primary production (Casotti et al., 2003; Siokou-Frangou et al., 2010; Civitarese et al., 2023).

The EMS is stratified continuously from May to October (D'Ortenzio et al., 2005). During the stratification period, primary production is reduced at the surface due to limited mixing with deeper, more nutrient-rich water, resulting in low surface Chla concentrations measured by satellites. Conversely, satellites measure highest Chla concentrations during winters, when surface-ocean cooling and winter storms bring deeper, nutrient-enriched waters towards the surface, fueling primary production. Nevertheless, the presence of a well-established deep chlorophyll maximum during the summer stratification period indicates that although satellites cannot detect it, primary production does occur deeper in the photic zone under these conditions (Boldrin et al., 2002; Casotti et al., 2003; Krom et al., 2003; Marañón et al., 2021). Hence, satellite Chla data mainly indicate variations in upper surface ocean production.

Consistent with the oligotrophic nature of the basin, the surface phytoplankton community in the EMS is dominated by picophytoplankton followed by nanoplankton (Siokou-Frangou et al., 2010). The nanoplankton community is dominated by coccolithophorids, mainly *G. huxleyi* (Siokou-Frangou et al., 2010), which are the main calcifying producers in the Mediterranean Sea (Ignatiades et al., 2009).

2.2 Sample collection and processing

Sinking particles were collected using a 0.5 m² sediment trap (KUM) deployed at 2340 m water depth during RV Pelagia cruise 64PE406 in the 3340-meter-deep Ionian Sea (34.96°, 18.04°). In

total, 40 samples were collected with a ten-day resolution spanning the time interval from 14 April 2017 to 19 May 2018. Prior to deployment, collection bottles were filled with filtered seawater (0.45 μm), poisoned with HgCl₂ (1.9 g L⁻¹) to prevent microbial degradation, and buffered with Borax (Na₂B₄O₇ · 10H₂O; 1.3 g L⁻¹). After retrieval during RV Pelagia cruise 64PE433 in August 2018, the bottles were transported and stored at the Royal NIOZ in the Netherlands at 4°C until further handling.

In the laboratory, supernatant was decanted, and large swimmers (>1mm) were removed by wet-sieving samples through a 1 mm mesh-size sieve. Next, the samples were wet-split in five aliquots using a WSD10 rotor splitter (McLane Laboratories) and washed with Millipore water, centrifuged, and decanted three times to remove salt, Borax buffer, and HgCl₂. Additionally, one 1/5th aliquot was split once more into 1/25th aliquots. Last, before storage until further analysis, three out of five 1/5th aliquots were freeze-dried immediately after splitting, and one 1/5th aliquot was stored with original supernatant containing HgCl₂ and Borax buffer for archive purposes. Two of the 1/25th aliquots were freeze-dried as well, the three remaining 1/25th splits were kept at 4°C for lithogenic analysis.

2.3 Bulk fluxes

Total mass flux (TMF) was determined by averaging the mass of two freeze-dried 1/5th aliquots of the total sample in pre-weighed vials. Total carbon (TC) and POC content (%wt), and stable organic carbon isotope ratios (δ¹³C) were analyzed using a Fisons Instrument NA 1500 elemental analyzer coupled to a Finnigan MAT Delta Plus isotope ratio mass spectrometer (IRMS). Samples for POC analysis were decalcified *in-situ* in silver sample cups according to Nieuwenhuize et al. (1994) by repetitive addition of 10-15 μl HCl (25%) followed by in-between drying steps until no further effervescence was noted. PIC content (%wt) was determined by subtracting POC from TC content.

2.4 Dust fluxes and grain-size distributions

To quantify the dust content and determine its particle-size distribution, the lithogenic fraction of two 1/25th aliquots was isolated by chemical removal of all biogenic material following McGregor et al. (2009). First, organic material was removed by oxidation with excess H₂O₂ (2 ml) in ~50 ml reversed osmosis (RO) water and boiling until all H₂O₂ has reacted. Second, biogenic carbonates were removed by adding excess HCl (2 ml, 10%) and boiling the mixture for exactly one minute. Third and finally, biogenic silica was removed by adding 2 g of NaOH pellets to the sample in 50 ml RO water and boiling for ten minutes. In between the different steps, RO water was added twice to a total volume of 1000 ml, and supernatant was decanted after allowing the suspended sediment to settle. The remaining lithogenic fraction can be considered dust, as atmospheric deposition of desert dust is the main source of terrestrial material into the EMS due to very limited river input (Guerzoni et al., 1999). Hence, mass and grain

size of the lithogenic fraction resemble dust mass and grain size. Although lithogenic carbonates may also be dissolved along with biogenic carbonates during the acidification step, marine biogenic carbonates are less resistant and are therefore dissolved first. Nonetheless, it is possible that the mass flux of the lithogenic fraction is slightly underestimated with this approach (Van der Does et al., 2016).

After chemical removal of all biogenic material, particle-size distributions were measured and masses of the remaining lithogenic (dust) fraction were obtained. Differences in modal grain size of the lithogenic particles in the sediment trap can be used to assess differences in dust provenance and transport. Particle-size distributions were measured with a Coulter laser diffraction particle sizer (LS13 320) with a micro liquid module (MLM). To prevent air-bubbles from altering the results, particles were suspended in degassed water during analysis and kept in suspension during analysis by using a magnetic stirrer. After particle-size distributions were acquired, the samples were filtered over pre-weighed polycarbonate filters (25 mm, 0.4 μm pore size) and reweighed to obtain dust masses.

2.5 Lipid biomarkers

Selected lipid biomarkers for higher plants, specific phytoplankton groups, and zooplankton were studied. Long-chain even-numbered *n*-alkanoic acids with a chain length of 26–32 carbon atoms are derived from epicuticular waxes from higher plants (Eglinton and Hamilton, 1963). Terrestrial plant waxes can enter the marine environment through riverine or aeolian input. As virtually no river input reaches the study site we interpret long-chain fatty acids (LCFAs) as indicators of aeolian (dust) input of terrestrial material. Dust-associated plant waxes can be derived from contemporary vegetation, soil organic matter, and remnants of ancient vegetation in sediments from paleolakes and playas (Eglinton et al., 2002). A range of lipids that are solely produced by phytoplankton are used to study changes in the composition of the phytoplankton community and the source of the organic matter exported associated with dust. Di- and tri-unsaturated C_{37} – C_{39} alkenones (long-chain alkenones) are produced by haptophyte species *G. huxleyi* (Volkman et al., 1980) and are therefore used as a biomarker for carbonate bearing coccolithophores. Long-chain C_{30} 1,15 diols are associated with marine eustigmatophytes including the *Nannochloropsis* genus (Rampen et al., 2012, 2022). Dinosterol or 4 α ,23,24-trimethylcholest-22E-en-3 β -ol is a major sterol in dinoflagellates, although not all species produce it (Volkman, 2016). Brassicasterol or 24 β -methylcholesta-5,22E-dien-3 β -ol is a common sterol in diatoms, although it is also found in prymnesiophytes (Volkman, 2016). As not all diatom species produce this compound and it mainly occurs in pennate diatoms as the major sterol (Rampen et al., 2010), we here use brassicasterol as non-comprehensive biomarker for diatom occurrence. Cholesterol (Cholest-5-en-3 β -ol) is a general compound in organic matter. High concentrations are usually associated with zooplankton and fecal pellets in oligotrophic open ocean regions (Gagosian and Nigrelli, 1979; Gagosian et al., 1980)

including the Mediterranean Sea (Gogou and Stephanou, 2004), and are therefore used as a marker for organic material derived from higher trophic levels in this study.

For lipid biomarker analysis, one 1/5th washed and freeze-dried aliquot from each sample was extracted in 25 ml dichloromethane (DCM):methanol (MeOH) (9:1, v:v) using microwave extraction (Milestone Ethos X). After extraction, total lipid extracts (TLEs) were passed over a small NaSO_4 column to remove any remaining water. Subsequently, the TLE was acid-hydrolyzed using 1.5N HCl in MeOH for 120 mins at 70°C and methylated using trimethylsilyl diazomethane to allow for analysis of fatty acids derived from wax esters. Next, samples were fractionated into apolar, neutral and polar fractions by eluting over a 4 cm AlO_3 column with hexane:DCM (9:1, v:v), hexane:DCM (1:1, v:v) and DCM: MeOH (1:1, v:v) respectively.

Prior to analysis, all fractions were dissolved in ethyl acetate before injection on-column into a gas chromatograph coupled to a flame ionization detector (GC-FID; Hewlett Packard 6890 series) equipped with a CP-Sil 5CB silica capillary column (25 m \times 0.32 mm, film thickness 0.12 μm). A known amount of squalane standard was added for quantification. Additionally, polar fractions were silylated by dissolving the sample in 10 μl pyridine and 10 μl N_2O -bis(trimethylsilyl) trifluoroacetamide (BSTFA) and heating for 20 minutes at 60°C. Samples were injected on-column at 70°C with helium as a carrier gas with a flow rate of 2 ml min^{-1} . Oven temperature increased with 20°C min^{-1} to 130°C and then with 4°C min^{-1} before being kept at 320°C for 10 minutes. To identify compounds of interest, several samples were also analyzed on a GC-mass spectrometer (GC-MS; Finnigan Trace GC Ultra, DSQ MS) with a similar column and heating program as the GC-FID.

2.6 Remote sensing oceanographic and atmospheric data

Time series of area-averaged remote sensing data for *Chla* (NASA Goddard Space Flight Center, 2022), sea surface temperature (SST) (JPL MUR MEaSUREs Project, 2015), precipitation (Huffman et al., 2016), and aerosol optical depth (AOD) (Platnick et al., 2015) were retrieved from the NASA Giovanni online data system. *Chla* and SST were obtained from a 1° \times 1° grid box around the sediment trap (17.7155 – 18.7155°N, 34.0783 – 35.0783°E) with the highest available temporal resolution of eight days from the Moderate Resolution Imaging Spectroradiometer (MODIS) Aqua satellite. Precipitation rate was retrieved for the same grid box from the Tropical Rainfall Measuring Mission Project (TRMM). AOD, which is a measure of radiation extinction due to aerosol scattering and absorption, was retrieved from a larger grid box (4° \times 4°) covering most of the Ionian Basin (16.5 – 20.5°N, 33.5 – 37.5°E) to decrease the chance of missing dust events due to too-low temporal resolution of the remote sensing coverage. AOD can be used as a proxy for atmospheric dust load, although it may also register other aerosols such as soot and volcanic ash. To ensure increased AOD values truly represent dust and not soot or ash, the potential dust events in the AOD record are visually compared to satellite images of the sediment trap region.

2.7 Principal component analysis

To assess the main factors of variance in particle fluxes over the studied interval a principal component analysis (PCA) was performed on the sediment-trap dataset using the R-Package Stats (version 3.6.2). 39 from the total 40 samples were included in the PCA; only sample 31 (08-02-2018 to 18-02-2018) was excluded because of missing POC and PIC fluxes due to very low particle flux. PCA was performed on normalized biomarker bulk fluxes (TMF, PIC, POC, and dust), lipid biomarker fluxes (LCFAs, long-chain alkenones, C₃₀ 1,15 diols, cholesterol, brassicasterol, and dinosterol), modal grain size of the dust fraction, and POC $\delta^{13}\text{C}$.

3 Results

3.1 Environmental conditions

SST and Chla changed seasonally over the studied interval, following patterns typical for the EMS: SST ranged from 15.2 °C to 29.5 °C, with maximum values in September 2017 and minimum values in February 2018 (Figure 1); Chla concentrations ranged from 0.045 mg m⁻³ in July 2017 to 0.243 mg m⁻³ in February 2018 and were generally low with high SSTs during the summer stratification period and high with low SSTs during the winter mixing period, when nutrients from deeper water layers reach the surface ocean. This seasonal pattern in Chla concentrations is typical for the EMS ‘non-blooming regime’ that is characterized by maximum Chla concentrations in winter (January-February) (D’Ortenzio and Ribera D’Alcalà, 2009).

Satellite AOD ranged from 0.02 to 1.18 (unitless) over the study period. Intervals with high AOD values (>0.5), corresponding to high aerosol concentrations and hazy skies, occurred several times throughout the year (Figure 1): from spring to early summer 2017,

in fall 2017, and from late winter to early summer 2018. AOD maxima during spring-early summer are in agreement with general patterns of dust transport above the central and eastern Mediterranean Sea: based on long-term remote sensing data, dust transport over the Ionian Basin follows a bimodal distribution with a first maximum in spring, and a second in summer (Moulin et al., 1998; Israelevich et al., 2012; Varga et al., 2014). However, increased AOD values in February 2018 (Figure 1) occurred relatively early compared to the 1997-2012 average, where AOD values only increased from March (Varga et al., 2014).

3.2 Sediment trap bulk particle fluxes

Patterns of TMF, i.e., total particle export, showed large seasonal differences (Figure 2). TMF ranged from 6-79 mg m⁻² d⁻¹. Continuously elevated TMF occurred in spring and early summer 2017 and in spring 2018. In fall and winter, TMF was generally lower, although one minor and one major peak occurred in September and November 2017, respectively. Dust fluxes ranged from 0.8 mg m⁻² d⁻¹ to 30 mg m⁻² d⁻¹ and were strongly correlated to TMF (R=0.94, p<0.001; Figure 3) and comprised a substantial part of TMF (7.0-66.5% of total flux, mean 27.7%; Figure 2), indicating a strong coupling between export of dust and total export. Overall, the timing of the dust export events that are captured by the sediment trap aligns well with known seasons of dust transport to the Ionian Basin: although dust was present in the sediment trap year-round, distinct dust export maxima mainly occur in spring and early summer.

The carbon flux, comprising POC and PIC, varied seasonally (Figure 2). POC fluxes ranged from 0.3 to 3.7 mg m⁻² d⁻¹ and POC content (%wt) varied between 1.2 and 8.6%. PIC fluxes ranged from 0 to 3.2 mg m⁻² d⁻¹ and PIC content (%wt) varied between 0-4.6%. Although both POC and PIC fluxes were significantly

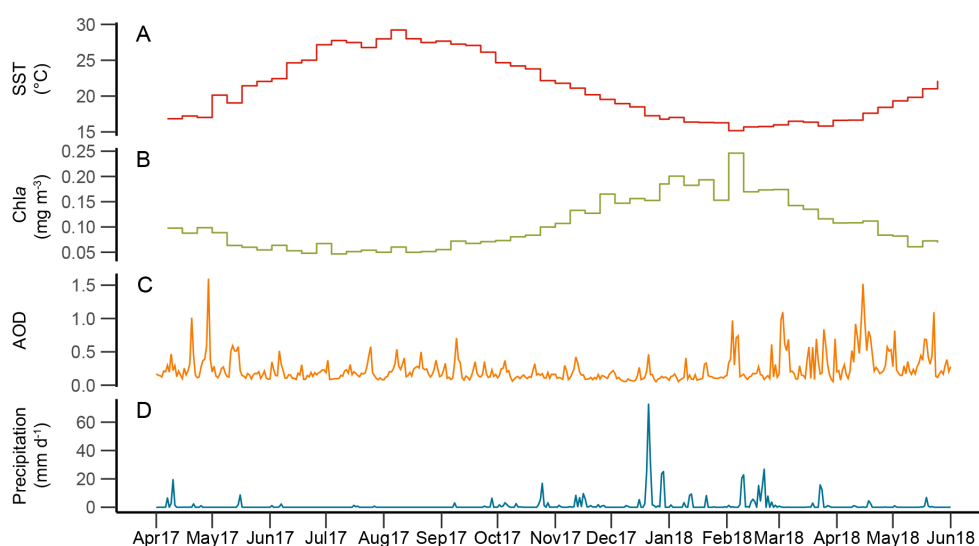


FIGURE 1

Time series of atmospheric and oceanographic remote sensing parameters: (A) sea surface temperature (SST; red); (B) surface ocean chlorophyll a concentration (Chla; green); (C) aerosol optical depth (AOD; orange); and (D) precipitation rate (blue).

correlated to TMF ($R = 0.8$ and 0.74 respectively, $p < 0.001$; Figure 3), the seasonal patterns deviate somewhat from the patterns in TMF and dust flux. Furthermore, the timing and shape of peak fluxes differed between POC and PIC. POC fluxes were highest during spring and early summer 2017, decreased towards late summer and remained low during the rest of the record, except for some minor peaks in fall 2017. In contrast, PIC

fluxes were more variable throughout the year and maximum fluxes occurred during a single export event in November 2017. Furthermore, POC export varied more gradually and in less distinctive peaks than the other bulk components. POC $\delta^{13}\text{C}$ values ranged from -22.0 to -26.0 ‰. On average, POC $\delta^{13}\text{C}$ is relatively negative in spring and summer 2017 and more positive during winter and autumn 2017 and spring 2018 (Figure 2).

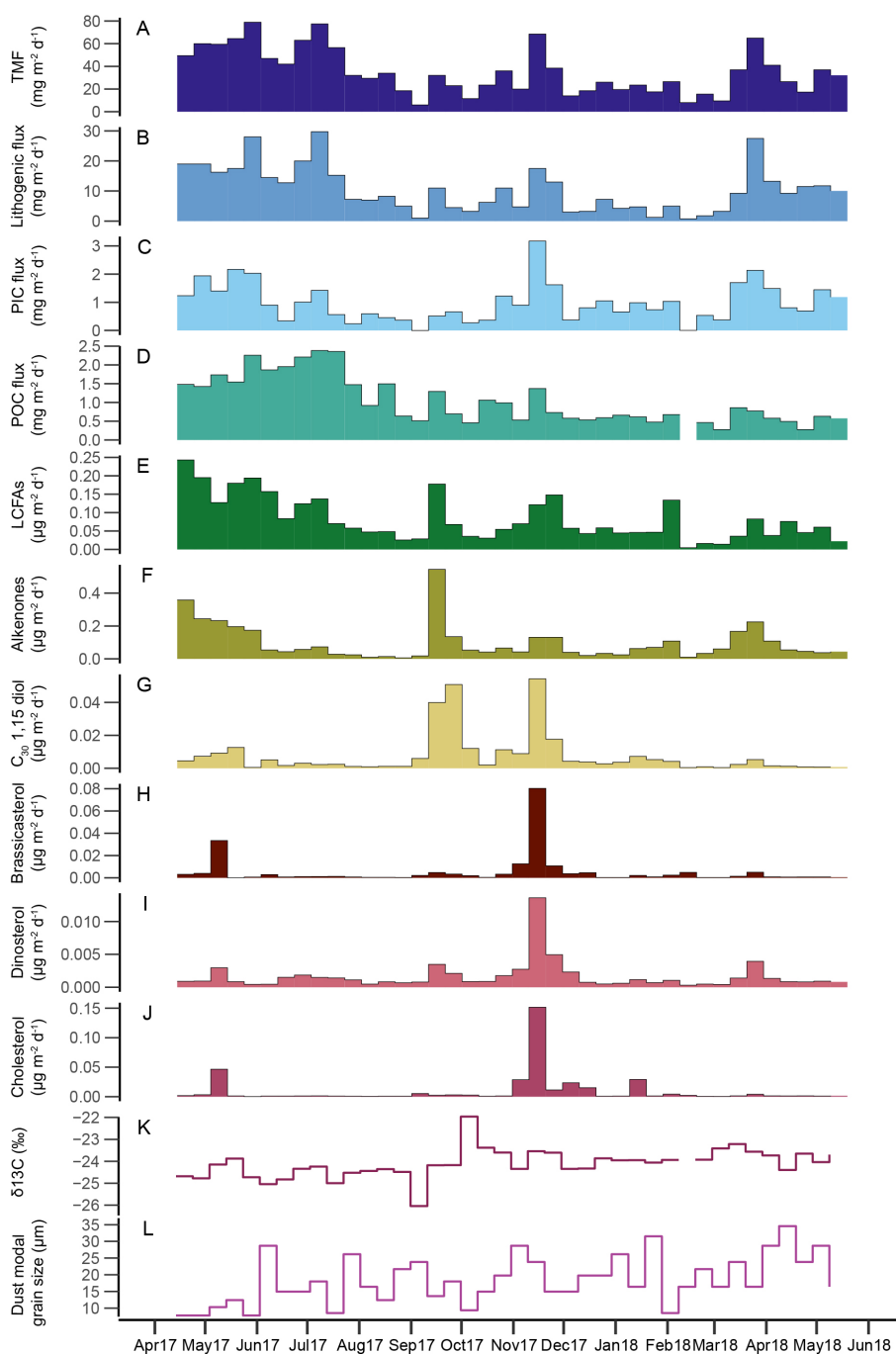


FIGURE 2

Time series of bulk fluxes (A–D), lipid biomarker fluxes (E–J), and parameters of settling particles (K, L) in the sediment trap: (A) total mass flux (TMF); (B) lithogenic material; (C) particulate inorganic carbon (PIC); (D) particulate organic carbon (POC); (E) long-chain fatty acids (LCFAs); (F) long-chain alkenones; (G) C_{30} 1,15 diols; (H) brassicasterol; (I) dinosterol; (J) cholesterol; (K) $\delta^{13}\text{C}$ of POC; and (L) modal grain size of the lithogenic fraction.

3.3 Dust characteristics

Modal grain size varied substantially over the one-year period ranging from 7.8 – 34.6 μm (median 16.4 μm , mean 18.5 μm). Most substantial differences occurred between spring 2017 and spring 2018 (Figure 2): where April and May 2017 were characterized by the smallest modal grain size of the studied interval, April and May 2018 were characterized by a relatively large modal grain size. Apart from this striking difference in grain size in spring between two consecutive years, variations in modal grain size seem to occur randomly over the study interval.

LCFA fluxes ranged from $<0.01 - 0.24 \mu\text{g m}^{-2} \text{d}^{-1}$. LCFAs generally followed the same pattern as dust fluxes ($R=0.68$; Figure 3), suggesting that plant waxes are indeed associated with dust deposition (Figure 2). However, some exceptions occurred. For example, plant wax fluxes were particularly high during a relatively minor dust export event in September 2017. In contrast, during the major dust event in March 2018, LCFA fluxes were relatively low. Dust entering the sediment trap in April-May 2017 has a ~fourfold higher plant fatty acid content than in April-May 2018. The variation in input of higher plant-derived lipids seems to coincide with differences in modal grain size: In general, dust events with relatively high LCFA fluxes are characterized by a small modal grain size (spring and summer 2017), whereas dust events with low LCFA fluxes (e.g., spring 2018) are characterized by a large modal grain size (Figure 2).

3.4 Marine lipid biomarker fluxes

Of the lipid biomarkers targeted in this study, long-chain alkenones, long-chain diols, dinosterol, and cholesterol have been detected in all samples. Brassicasterol was detected in all samples except one sample in February 2018. Alkenones were the dominant biomarker in most samples with fluxes ranging from $<0.001 - 0.54 \mu\text{g m}^{-2} \text{d}^{-1}$. Cholesterol fluxes ranged from $0.01 - 0.15 \mu\text{g m}^{-2} \text{d}^{-1}$, brassicasterol from 0 (not detected) – $0.080 \mu\text{g m}^{-2} \text{d}^{-1}$, dinosterol from $<0.001 - 0.014 \mu\text{g m}^{-2} \text{d}^{-1}$ and long-chain diols from $<0.001 - 0.054 \mu\text{g m}^{-2} \text{d}^{-1}$. Fluxes of all targeted biomarkers generally follow patterns of TMF (Figure 2). However, maximum fluxes differed in timing between biomarkers: long-chain alkenone fluxes peaked during a short-lived event in September 2017; brassicasterol, dinosterol, and cholesterol peaked in November 2017; and C_{30} 1,15 diols peaked both in September, together with the alkenones, and in November 2017 together with the sterols (Figure 2). Additionally, long-chain alkenone fluxes showed a second maximum with longer-sustained high fluxes in spring 2017 and 2018, although spring 2017 fluxes were substantially larger than spring 2018 fluxes. Alkenone fluxes decreased during summer 2017 and remained generally low until spring 2018, except for during the export event in September. Fluxes of the targeted sterols and C_{30} 1,15 diols were generally low throughout the year, apart from short-term episodes with increased fluxes in April-May 2017 and March-April 2018, although these fluxes were substantially lower than

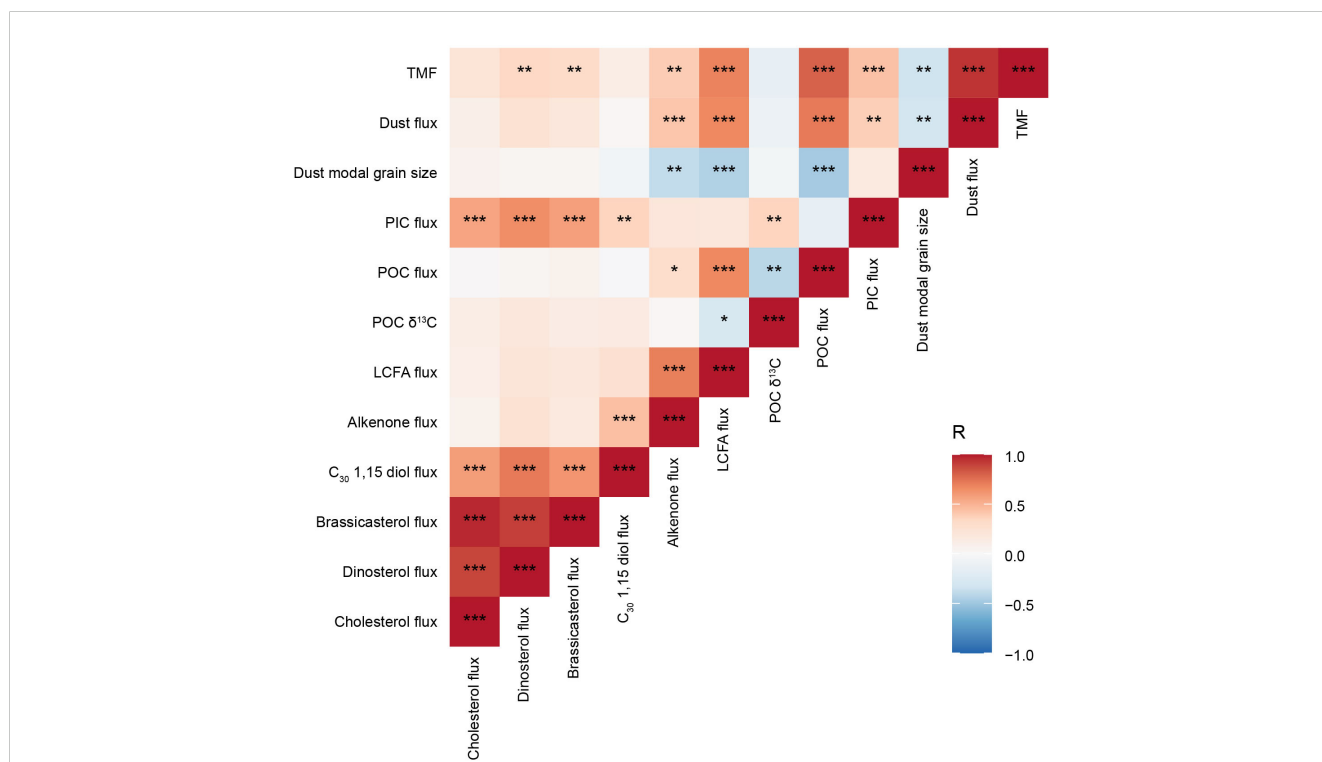


FIGURE 3 Heatmap of Pearson correlation of sediment-trap fluxes and parameters from Figure 2. Asterisks represent significance levels of 0.1 (*), 0.05 (**) and 0.01 (***). Blue colors represent negative correlations, and red colors represent positive correlations.

those during the maximum flux events in November 2017, and in September and November 2017, respectively.

Similar flux patterns of the targeted sterols are reflected by strong correlations between the sterols (all $R > 0.9$, $p < 0.001$; Figure 3). The correlation between the sterols and C_{30} 1,15 diols was less strong, but still significant ($R > 0.59$, $p < 0.001$). Alkenone and C_{30} 1,15 diols were also significantly correlated ($R = 0.45$, $p < 0.01$). However, alkenone fluxes were not significantly correlated to the sterol fluxes ($R < 0.25$).

3.5 Principal component analysis

The first three axes of the PCA together explain 76.7% of the variance of the data. Principal component (PC) 1 explains 41.3% of the variance. All biomarker and bulk fluxes score positively on PC1,

together with high-particle flux samples; Only modal grain size of the dust fraction scores negatively, together with low particle flux samples (Figure 4). PC2 explains 24.8% of the variance of the data. Sterol fluxes, C_{30} 1,15 diol fluxes, modal grain size, and POC $\delta^{13}C$ score positively, while bulk particle fluxes, alkenones, and long-chain fatty acids score negatively. On PC2, high-flux samples with high TMF, POC and alkenone fluxes, and a small modal grain size, plot negatively; only the November 2017 dust event characterized by a large modal grain size and high sterol and diol fluxes plots clearly positively. All low-flux samples score low positive or negative values. PC3 explains another 10.5% of the data. Modal grain size, POC and TMF fluxes, sterol fluxes, and to a lesser extent dust and PIC fluxes, score positively, while long-chain fatty acids, diols, and alkenones score negatively. PC3 separates samples with high TMF, dust and POC fluxes, and low LCFA fluxes from samples with a small modal grain size, high alkenone and high LCFA fluxes

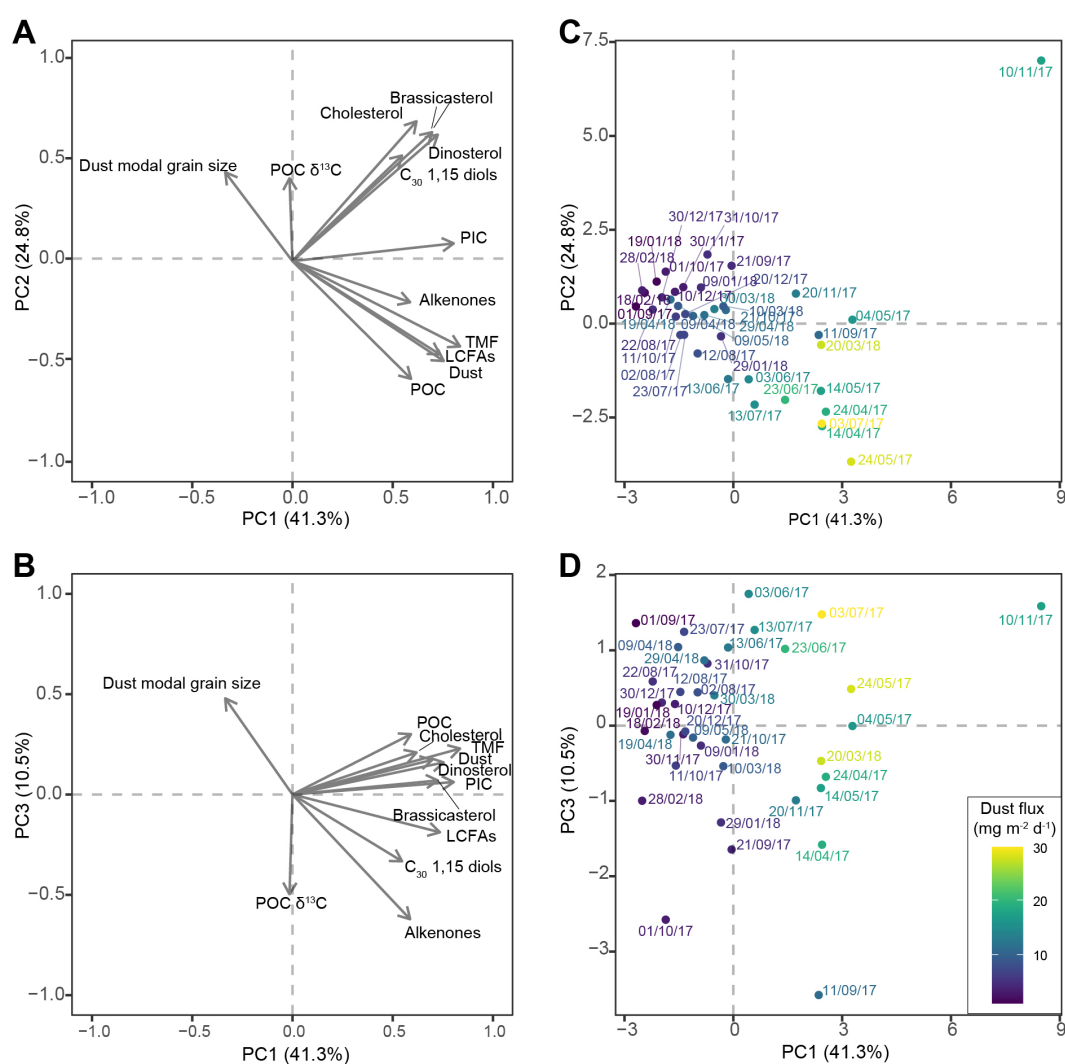


FIGURE 4

Principal component analysis (PCA) results of bulk and lipid biomarker fluxes and parameters of settling particles of the sediment-trap time series: (A, B) scores of TMF, dust, POC, PIC, long-chain fatty acids (LCFAs), long-chain alkenones (alkenones), C_{30} 1,15 diols, brassicasterol, dinosterol and cholesterol fluxes, modal grain size of the dust fraction, and POC $\delta^{13}C$ of principle component (PC) 1 and PC2, and PC1 and PC3, respectively, represented by grey arrows; (C, D) scores of the individual samples on PC1 and PC2, and PC1 and PC3, respectively, with sample labels indicating the start date of the sampling interval, and colors representing dust flux of the sample.

with a low POC and TMF flux, with a particularly negative score for the September 2017 dust event.

4 Discussion

4.1 Atmospheric dust outbreaks

Several dust events in the sediment trap can be distinguished based on increased dust and/or LCFA fluxes: two longer-sustained (4–6 weeks) dust events in spring and summer 2017, two short-lived (1–2 weeks) dust events in September and November 2017, and a longer-sustained (4 weeks) dust event again in spring 2018 (Figure 2). The dust events recorded by the sediment trap can be coupled to atmospheric dust outbreaks visible on satellite images (Supplementary Figure S1) assuming that the deposited dust is exported immediately and sinks at a rate of 70–200 m d⁻¹, as is established for the EMS (Patara et al., 2009; Malinverno et al., 2014). As a result, dust collected by the sediment trap at 2340 m water depth should be preceded by atmospheric dust occurrence ~10 to 30 days earlier. Indeed, increased AOD values (>0.5; Figure 1) and satellite images reveal dust clouds passing the Ionian basin in the expected time window (Supplementary Figure S1). However, not all occasions of increased AOD values are coupled to increased dust fluxes in the sediment trap, suggesting that the presence of dust in the atmosphere above the EMS does not always lead to its deposition. For example, deposition might be dependent on precipitation. Alternatively, it is possible that deposited dust is not exported to depth directly but remains suspended in the surface ocean to some extent. Nevertheless, since most of the dust events can be coupled to atmospheric dust outbreaks, it is likely that dust is exported rapidly upon deposition and does not remain suspended in the surface ocean for a substantial amount of time.

4.2 Carbon export in the eastern Mediterranean Sea

Export of organic material in oligotrophic ocean regions is hypothesized to be driven by ballasting of mineral particles, either dust or marine biogenic silicate or carbonate (Armstrong et al., 2002; Guerreiro et al., 2021), and zooplankton fecal pellets (Ploug et al., 2008). The strong correlations between TMF, dust flux, and to a lesser extent POC and PIC flux (Figure 3), indicate that export of the different bulk components is closely related. Intervals with high POC, PIC, and phytoplankton biomarker export occur out-of-sync with maximum surface primary productivity as indicated by *Chla* concentrations (Figure 1; Figure 2). This difference in seasonal patterns suggests that carbon export at the study site is decoupled from surface productivity, as has also been observed before at other locations in the eastern (Patara et al., 2009; Stavrakakis et al., 2013; Gogou et al., 2014; Pedrosa-Pamies et al., 2021) and western (Lee et al., 2009a; Ternon et al., 2010) Mediterranean Sea. Instead, the particularly strong correlation between dust and total export suggests that ballasting by dust particles drove particle export during the study period. Notably, although all POC export events

are also associated with increased terrigenous input, i.e., high dust and/or LCFA fluxes, not all dust events coincide with increased POC export (Figure 2). For example, dust events during spring 2017 are not accompanied by a substantial increase in POC export. A lack of POC export during dust events might be due to the absence of substantial POC in the surface ocean at time of dust deposition and no fertilizing effect of the deposited dust, or the absence of a ballasting effect by dust particles.

In addition to this overall relationship between dust deposition and carbon export, carbonate ballasting and zooplankton fecal pellets might contribute to enhanced POC export together with dust ballasting during specific events. The dust event in November 2017 that is associated with enhanced export of brassicasterol and C₃₀ 1,15 diols is also characterized by high cholesterol and carbonate fluxes (Figure 2). Hence, increased export biomarker export during this event might have been driven by a combination of dust fertilization, zooplankton grazing, and mineral ballasting by dust and carbonate particles.

4.3 Molecular composition of exported POC

The occurrence and composition of lipid biomarkers in the sediment trap material can be used to further assess the source(s) of the biogenic particles that are exported. The distinct trends in the biomarker occurrence indicate that the response and/or export of different phytoplankton groups varies between dust events (Figure 2). This varying response to dust deposition between phytoplankton groups throughout the year can be explained by two main mechanisms: either ballasting by dust particles increases export of the phytoplankton community already present in the surface ocean prior to dust deposition, or dust fertilization changes the composition of the phytoplankton community, which can benefit different phytoplankton groups during different events based on the season of dust deposition and characteristics of the deposited dust. Since the sediment trap was located well below the photic zone in the deep EMS, our results can mainly give insight into the effects of dust on carbon export and not productivity, as it records an export signal. However, fertilizing effects of dust can indirectly be assessed by comparing the exported phytoplankton biomarkers to the expected phytoplankton community composition of the specific dust events.

Export of all targeted phytoplankton biomarkers increases substantially during the dust events in spring 2017 and, to a lesser extent, 2018, reflecting the presumably diverse phytoplankton composition of the phytoplankton community present after the late winter peak in surface ocean productivity (Figure 2). The lipid biomarker composition in the trap during spring resembles that observed by Pedrosa-Pamies et al. (2021) during spring 2011–2013, suggesting that this community is characteristic for the open EMS during this season. Furthermore, sustained high fluxes of long-chain alkenones in the sediment trap during spring-early summer 2017 also concur with known seasons of high coccolithophore and in particular *G. huxleyi* abundance in the Ionian Sea (Casotti et al., 2003; Ignatiades et al., 2009; Varkitzi et al., 2020) and coincide with

intervals of maximum coccolith export (Malinverno et al., 2009, 2014, Skampa et al., 2020). Given the resemblance of the exported biomarkers with the typical seasonal occurrence of their source organisms in the EMS, the biomarker distributions do not provide a clear indication for dust fertilization during spring. This contrasts with the dust event in September 2017, when long-chain alkenones and C₃₀ 1,15 diols, related to the coccolithophore *G. huxleyi* and eustigmatophytes, respectively, are exported in relatively higher abundances than other phytoplankton markers. Although coccolithophore abundance in the EMS peaks during late summer-autumn in addition to spring (Malinverno, 2003; Siokou-Frangou et al., 2010), alkenone producer *G. huxleyi* is generally less abundant during this time of year due to lower nutrient availability compared to during spring (Knappertsbusch, 1993). *G. huxleyi* is an opportunistic coccolithophore species that is known to benefit from temporarily relieved nutrient limitation, and increased *G. huxleyi* abundance can be the result of vertical mixing, but also of dust deposition (Malinverno et al., 2009; Guerreiro et al., 2023). Therefore, the elevated alkenone flux during the September 2017 dust event could be the result of dust fertilization. Nonetheless, the simultaneously high C₃₀ 1,15 diol fluxes coincide with the known seasonality of eustigmatophytes in the WMS where maximum eustigmatophyte abundance occurs during maximum stratification in August (Rampen et al., 2022). Hence, the increased C₃₀ 1,15 diol fluxes could also point towards a ballasting mechanism during this event.

Another example of potential dust fertilization occurs during the dust event in November 2017. The peak fluxes of brassicasterol and dinosterol during this event indicate enhanced export of diatom- and dinoflagellate-derived material, together with another peak in eustigmatophyte-derived C₃₀ 1,15 diol export. Although diatoms and dinoflagellates occur year-round in the EMS, they are usually relatively low in abundance (Boldrin et al., 2002; Varkitzi et al., 2020). In the Ionian basin, an increased abundance of these species groups is typically associated with production deeper in the photic zone during summer, when nutrient concentrations in the surface ocean are lowest and light can penetrate deeper into the water column (Malinverno, 2003; Varkitzi et al., 2020). Additionally, a (temporary) relief in nutrient limitation due to strong mixing can lead to an increase in diatom production in the surface ocean in the Mediterranean Sea (Casotti et al., 2003; Varkitzi et al., 2020). However, the peak in brassicasterol flux in November 2017 occurs too early in the mixing period as sufficiently strong mixing that allows for diatom blooms usually only occurs later in the mixing period in the Mediterranean Sea, from January to March (Marty et al., 2002; Reich et al., 2022). This suggests that increased export of phytoplankton biomarkers during the November dust event might be a result of increased productivity and a change in phytoplankton community composition due to dust fertilization, possibly enhanced by the onset of the winter mixing period resembled by an increase in surface Chl_a concentrations (Figure 1). Increased cholesterol fluxes, derived from zooplankton and fecal pellets (Figure 2), also point towards increased production. Additionally, fecal pellets, carbonate ballasting, and dust ballasting might have increased vertical export during this event, as suggested earlier (see section 4.2).

4.4 Different types of dust

One explanation for the observed differences in the export of biogenic material between dust events is that the properties of the deposited dust vary between dust events. Large differences in modal grain size through the studied interval support the occurrence of different types of dust. Based on LCFA content and modal grain size at least two types of dust can be distinguished: one type with a small modal grain size and more plant material, as is dominant in spring 2017, and one with a larger modal grain size and less plant material, as is dominant in November 2017 and spring 2018 (Figure 2). These two dust types are also discriminated by the PCA, as PC2 separates the spring 2018 and November 2017 dust events with a large modal grain size and low LCFA fluxes from dust events with a small modal grain size and high LCFA fluxes and POC fluxes, i.e., the spring 2017 dust events (Figure 4).

Dust transported to the Mediterranean Sea can be derived from varying sources in the north African deserts, such as playas and lakebeds (Prospero et al., 2002; Tegen et al., 2002) or from sand dunes (Crouvi et al., 2012). Dust derived from playas and dried-up lake beds are associated with finer-grained dust that translates into a relatively large surface area. In principle, the larger surface area of small particles allows them to carry relatively more nutrients compared to larger-sized particles, thereby increasing their potential fertilizing capacity. Furthermore, fine dust from dried-up river and lake beds likely also contains more organic material. The finer, LCFA-rich dust deposited during spring 2017 is associated with a much stronger increase in POC export compared to the coarser dust deposited in November 2017 and spring 2018, which corresponds with the presumed fertilizing potential of the different dust types.

To assess whether these two dust types are derived from different sources, NASA Worldview satellite images of dust events were inspected (MODIS Aqua and Terra Corrected Reflectance imagery). Furthermore, back trajectories of air masses present over the sediment trap site during atmospheric dust events were estimated using the NOAA HYSPLIT transport and dispersion model (Stein et al., 2015; Rolph et al., 2017). As dust transport over the Mediterranean Sea is often multilayered and occurs between 1.5 to 5 km altitude, particles were backtracked at 1500, 3000, and 5000 meter above sea level (masl). Additionally, back trajectories for 500 m altitude were generated, as dust clouds originating from northeast (NE) Libya visible on satellite images mainly seemed to be transported at lower altitudes. Based on the generated back trajectories, three main dust transport routes and sources can be distinguished: one originating in NE Libya, one passing over northern Algeria and Tunisia, and one passing over southern Algeria and western and central Libya (Supplementary Figure S1). The first transport route is visible as clear, long and narrow dust plumes along the Libyan coast on the satellite images and indicates a proximal dust source (Supplementary Figure S1). Dust from this region is mainly derived from a small area in NE Libya consisting of wadis and associated complexes of salt and dry lakes (Prospero et al., 2002; Koren et al., 2003). The latter two dust transport paths are visible as large dust clouds that are transported north-eastward from North Africa (Supplementary Figure S1). Both transport

routes pass multiple known dust sources, where the northern route passes over salt lakes ('chots'), dry lakes, and alluvial deposits in northeast Algeria and Tunisia that are mainly composed of fine-grained dust, and the southern route passes over known dust sources in southern Algeria (Ahaggar region) and the central Libyan desert (Prospero et al., 2002; Scheuven et al., 2013). The relatively coarse dust deposited in November 2017 and spring (April-May) 2018 seems to be transported at 500 m altitude from NE Libya, combined with dust from eastern/central Libya and southern Algeria. In turn, dust deposited during spring 2017 is characterized by a very small modal grain size (Figure 2) and seems mainly to be sourced from Tunisia and northern Algeria. Nevertheless, dust derived from different sources can simultaneously be transported by different wind systems at various altitudes (Hamonou et al., 1999). Hence, the dust deposited during one event can consist of a mixture of multiple sources. Satellite images and back trajectories also often show transport from multiple sources during dust events. Therefore, it remains difficult to pinpoint specific source areas of these dust transport pathways for most dust events, and radiogenic isotopes of the dust are necessary to constrain the exact dust sources.

In addition to the modal grain size of the deposited dust, varying fertilization effects between dust events might also be a result of differences in deposition mode, i.e., wet or dry. The dust event in November 2017 is likely to be associated with wet deposition, as the peak in AOD associated with this dust event coincides with (a small amount of) precipitation (Figure 1). Hence, wet deposition could explain the apparent fertilizing effect of this dust event discussed in section 4.3 despite the relatively large grain size of the deposited dust. However, different deposition modes alone cannot explain differences between the dust events of spring 2017 and spring 2018 as during both years, some occurrences of increased AOD coincide with increased precipitation, but others do not (Figure 1).

In addition to dust deposition, deposition of other aerosols might also have had a fertilizing effect. Satellite images reveal that the increase in dust and TMF in September 2017 coincides with not only a dust cloud, but also with smoke clouds passing over the sediment trap area (Supplementary Figure S1). Despite the relatively minor increase in dust flux, this event is characterized by high LCFA fluxes, suggesting substantial terrestrial input (Figure 2). This difference between LCFA-associated export during September 2017 and dust-associated export during the other export events is also captured by PC3 of the PCA, which separates export events with high dust and POC fluxes from export events associated with low dust flux but high LCFA, alkenone, and diol fluxes, in particular the September 2017 dust event (Figure 4). The smoke cloud could be visually traced back to North America, where large-scale wildfires occurred a week prior to the arrival of the smoke plume to the Ionian Basin. HYSPLIT back trajectories confirm movement of air masses from the USA to the Mediterranean Sea with the jet stream during late August – early September (Supplementary Figure S1). The occurrence of high long-chain alkenone and C₃₀ 1,15 diol fluxes during this interval suggest that smoke aerosols, possibly together with north African

dust deposition, can also stimulate export of eustigmatophyte and haptophyte phytoplankton material, either through fertilization or ballasting (see section 4.3).

4.5 Implications for the strength of the carbon pump

Although POC export in the sediment trap is associated with dust deposition, the effect of dust on the biological carbon pump depends on the source of exported POC. When dust deposition is associated with export of *in-situ* produced material, i.e., contemporary marine POC, increased POC export results in a net sequestration of carbon. However, when dust deposition is mainly associated with export of pre-aged terrestrial POC, there is no net effect on the carbon pump.

Average $\delta^{13}\text{C}$ values of -24.1 ‰ for POC in the sediment trap are relatively low for an open marine system given that marine phytoplankton usually has $\delta^{13}\text{C}$ values of -22 to -18 ‰ (Goericke and Fry, 1994). Similar $\delta^{13}\text{C}$ values (~-24‰) are also found for seafloor sediments in the Ionian Basin (Pedrosa-Pàmies et al., 2015) and settling POC in sediment traps in the nearby Ierapetra basin (Pedrosa-Pàmies et al., 2021). Notably, the sediment in the central Ionian Sea has particularly low POC $\delta^{13}\text{C}$ values compared to other EMS sites, where $\delta^{13}\text{C}$ is ~-18 to -24‰ (Pedrosa-Pàmies et al., 2015). These relatively low values have been explained by substantial contributions of terrestrial and anthropogenic carbon to the sedimentary POC pool (Pedrosa-Pàmies et al., 2015; Pedrosa-Pàmies et al., 2021), which is supported by relatively high terrestrial n-alkane concentrations in the Ionian basin sediments compared to other EMS sites (Pedrosa-Pàmies et al., 2015). This suggests that the relatively low $\delta^{13}\text{C}$ values for the POC in the sediment trap are also related to the input of terrestrial plant material. In particular vegetation following the C3 pathway for CO₂ fixation has $\delta^{13}\text{C}$ values ranging from -25 to -28 ‰ (Hedges et al., 1997). A substantial contribution of C3 vegetation to exported POC in the EMS is remarkable as the sparse vegetation in the Saharan desert, an important source of dust, is dominated by C4 vegetation of which $\delta^{13}\text{C}$ values are comparable to that of marine OC. However, North-African vegetation in the band around the Mediterranean Sea is dominated by C3 plants (Still and Powell, 2009), which could be the source of low $\delta^{13}\text{C}$ POC to the trap. Furthermore, playas or desiccated lake beds can store remnants of ancient C3 vegetation, which can be transported to the trap together with the dust from these areas (Eglinton et al., 2002). Similarly, contributions of anthropogenic carbon could lower POC $\delta^{13}\text{C}$, as $\delta^{13}\text{C}$ values for crude oil or petroleum are around -28.5 ‰ (Rumolo et al., 2011). Although input of allochthonous POC from terrestrial vegetation or anthropogenic sources likely contributes to the exported POC in the sediment trap and reduces the apparent effect of dust deposition on the biological pump, variation in POC $\delta^{13}\text{C}$ is relatively minor throughout the year and between dust events (Figure 2).

The net effect of dust deposition on the biological pump further depends on the relative amounts of POC export, which stimulates the biological pump, and PIC export, which stimulates the

carbonate counter pump. Although both POC and PIC export are each significantly correlated to dust flux (Figure 3), the amount of POC export relative to that of PIC varies between dust events. Most dust events are associated with increased fluxes in both PIC and POC. This indicates that dust-driven export of biogenic material does not necessarily result in increased carbon sequestration. Only the September export event, likely driven by a combination of fertilization and ballasting by wildfire smoke aerosols and dust (see section 4.3), is not associated with increased PIC export. However, the effect of this event on the biological pump is small, as it is only associated with a slight increase in POC flux (Figure 2). Dust events characterized by dust with a large modal grain size, e.g., during November 2017 and spring 2018, seem to be associated with strengthening of the carbonate counter pump instead of the biological pump as the increase in PIC export is much larger than POC export during these events (Figure 2). Conversely, dust events with a smaller modal grain size, e.g., the spring 2018 dust event, are associated with a relatively larger increase in POC export. Hence, the net effect of dust deposition on the biological pump might be associated with compositional changes of the deposited dust: smaller dust particles are associated with strengthening of both the biological carbon pump and the carbonate counter pump, whereas larger dust particles are mainly associated with enhanced strength of the carbonate counter pump. Additionally, the effects of dust deposition on the biological pump also vary interannually as indicated by differences in the relative increase of POC and PIC fluxes between spring 2017 and 2018 (Figure 2).

5 Conclusions

We have compared fluxes of sinking particles comprising mineral dust, marine biogenic carbon, and source-specific phytoplankton biomarkers from a sediment-trap mooring deployed from April 2017 – May 2018 to study the relationships between dust deposition and organic carbon export in the eastern Mediterranean Sea. Several dust events occur throughout the studied period, and dust export events in the sediment trap at 2340 m water depth can be coupled to dust outbreaks in the atmosphere occurring 10–30 days earlier. Our findings suggest that dust is an important driver for carbon export as all intervals of increased biogenic particle fluxes coincide with dust events. However, not all dust events are associated with increased POC export, and the carbon sequestering role of dust seems to be limited to specific events. Although increased export fluxes of phytoplankton biomarkers are also associated with dust events, the composition varies between events. Overall, dust events seem to have differing effects on the export of biogenic material based on compositional changes of the deposited dust that are reflected by variation in grain size distribution. We find that fine dust deposited in spring 2017 resulted in a small increase in POC and phytoplankton biomarker export, but not in a change in phytoplankton community composition. Conversely, coarser dust deposited in November 2017 is associated with a change in phytoplankton community composition indicating a fertilizing

effect of the deposited dust. However, deposition of relatively coarse dust during dust events in November 2017 and spring 2018 is mainly associated with increased PIC instead of POC export, and therefore results in a net decrease of carbon sequestration through the carbonate counter pump. The only dust event that is associated with increased POC export and a change in phytoplankton community composition indicating fertilization coincides with smoke clouds from large-scale wildfires in North America, suggesting that fertilizing and ballasting effects during this event might have been a combination of deposition of dust and smoke aerosols. For a better understanding of the effects of the season of dust deposition on the biological pump and potential interannual variability in dust transport and natural phytoplankton dynamics, it is essential to study multi-year time series of dust deposition and biogenic export. Furthermore, as the findings of this study are restricted to one sediment trap of 2340 m water depth, it is difficult to distinguish fertilizing from ballasting effects of dust. To better separate these effects, it is essential to study organic matter export at different water depths.

Data availability statement

The original contributions presented in the study are publicly available. This data can be found here: <https://doi.org/10.25850/nioz/7b.b.cj>.

Author contributions

AB: Conceptualization, Data curation, Formal Analysis, Investigation, Methodology, Project administration, Validation, Visualization, Writing – original draft. J-BS: Conceptualization, Funding acquisition, Investigation, Methodology, Resources, Supervision, Writing – review & editing. FP: Conceptualization, Funding acquisition, Investigation, Methodology, Resources, Supervision, Writing – review & editing.

Funding

The author(s) declare that financial support was received for the research, authorship, and/or publication of this article. This project was funded by the UU-NIOZ project “Unravelling seasonal dust-induced productivity changes in the Mediterranean Sea” (project nr. NZ4543.28), funded by Utrecht University.

Acknowledgments

We thank captains and ship crews as well as scientific crews of RV Pelagia expeditions 64PE418 and 64PE443 for deployment and recovery of the sediment trap. We also thank Klaas Nierop and Desmond Eefting for their assistance in the lab and Reinout van Riel for assisting splitting and processing of the sediment trap samples.

The authors gratefully acknowledge the NOAA Air Resources Laboratory (ARL) for the provision of the HYSPLIT transport and dispersion model and READY website (<https://www.ready.noaa.gov>) used in this publication. Analyses used in this paper were produced with the Giovanni online data system, developed and maintained by the NASA GES DISC. We also acknowledge the MODIS mission scientists and associated NASA personnel for the production of the data used in this research effort. We further acknowledge the use of imagery from the Worldview Snapshots application (<https://wvs.earthdata.nasa.gov>), part of the Earth Observing System Data and Information System (EOSDIS). We also thank the editor and the reviewers for their feedback on an earlier version of this work.

Conflict of interest

The authors declare that the research was conducted in the absence of any commercial or financial relationships that could be construed as a potential conflict of interest.

References

- Antoine, D., André, J.-M., and Morel, A. (1996). Oceanic primary production: 2. Estimation at global scale from satellite (Coastal Zone Color Scanner) chlorophyll. *Global Biogeochem. Cycles* 10, 57–69. doi: 10.1029/95gb02832
- Armstrong, R. A., Lee, C., Hedges, J. I., Honjo, S., and Wakeham, S. G. (2002). A new, mechanistic model for organic carbon fluxes in the ocean based on the quantitative association of POC with ballast minerals. *Deep Sea Res. Part II: Topical Stud. Oceanogr.* 49, 219–236. doi: 10.1016/S0967-0645(01)00101-1
- Boldrin, A., Miserocchi, S., Rabitti, S., Turchetto, M., Balboni, V., and Socal, G. (2002). Particulate matter in the southern Adriatic and Ionian Sea: characterisation and downward fluxes. *J. Mar. Syst.* 33, 389–410. doi: 10.1016/S0924-7963(02)00068-4
- Bressac, M., Guieu, C., Doxaran, D., Bourrin, F., Desboeufs, K., Leblond, N., et al. (2014). Quantification of the lithogenic carbon pump following a simulated dust-deposition event in large mesocosms. *Biogeosciences* 11, 1007–1020. doi: 10.5194/bg-11-1007-2014
- Casotti, R., Landolfi, A., Brunet, C., D'Ortenzio, F., Mangoni, O., Ribera D'Alcalá, M., et al. (2003). Composition and dynamics of the phytoplankton of the Ionian Sea (eastern Mediterranean). *J. Geophys. Res.: Oceans* 108, 8116. doi: 10.1029/2002jc001541
- Civitaresse, G., Gačić, M., Batistić, M., Bensi, M., Cardin, V., Dulčić, J., et al. (2023). The BiOS mechanism: History, theory, implications. *Prog. Oceanogr.* 216, 103056. doi: 10.1016/j.pocean.2023.103056
- Civitaresse, G., Gačić, M., Lipizer, M., and Eusebi Borzelli, G. L. (2010). On the impact of the Bimodal Oscillating System (BiOS) on the biogeochemistry and biology of the Adriatic and Ionian Seas (Eastern Mediterranean). *Biogeosciences* 7, 3987–3997. doi: 10.5194/bg-7-3987-2010
- Crouvi, O., Schepanski, K., Amit, R., Gillespie, A. R., and Enzel, Y. (2012). Multiple dust sources in the Sahara Desert: The importance of sand dunes. *Geophys. Res. Lett.* 39, L13401. doi: 10.1029/2012gl052145
- D'Ortenzio, F., Iudicone, D., De Boyer Montegut, C., Testor, P., Antoine, D., Marullo, S., et al. (2005). Seasonal variability of the mixed layer depth in the Mediterranean Sea as derived from *in situ* profiles. *Geophys. Res. Lett.* 32, L12605. doi: 10.1029/2005gl022463
- D'Ortenzio, F., and Ribera D'Alcalá, M. (2009). On the trophic regimes of the Mediterranean Sea: a satellite analysis. *Biogeosciences* 6, 139–148. doi: 10.5194/bg-6-139-2009
- Eglinton, G., and Hamilton, R. (1963). "The distribution of alkanes," in *Chemical plant taxonomy*. Ed. T. Swain (Academic Press, London), 187–218.
- Eglinton, T. I., Eglinton, G., Dupont, L., Sholkovitz, E. R., Montluçon, D., and Reddy, C. M. (2002). Composition, age, and provenance of organic matter in NW African dust over the Atlantic Ocean. *Geochem. Geophys. Geosys.* 3, 1–27. doi: 10.1029/2001gc000269
- Gačić, M., Borzelli, G. L. E., Civitaresse, G., Cardin, V., and Yari, S. (2010). Can internal processes sustain reversals of the ocean upper circulation? The Ionian Sea example. *Geophys. Res. Lett.* 37, L09608. doi: 10.1029/2010gl043216
- Gagosian, R. B., and Nigrelli, G. E. (1979). The transport and budget of sterols in the western North Atlantic Ocean. *Limnol. Oceanogr.* 24, 838–849. doi: 10.4319/lo.1979.24.5.0838
- Gagosian, R. B., Smith, S. O., Lee, C., Farrington, J. W., and Frew, N. M. (1980). Steroid transformations in Recent marine sediments. *Phys. Chem. Earth* 12, 407–419. doi: 10.1016/0079-1946(79)90122-8
- Gazeau, F., Ridame, C., Van Wambeke, F., Alliouane, S., Stolpe, C., Irissou, J.-O., et al. (2021a). Impact of dust addition on Mediterranean plankton communities under present and future conditions of pH and temperature: an experimental overview. *Biogeosciences* 18, 5011–5034. doi: 10.5194/bg-18-5011-2021
- Gazeau, F., Van Wambeke, F., Marañón, E., Pérez-Lorenzo, M., Alliouane, S., Stolpe, C., et al. (2021b). Impact of dust addition on the metabolism of Mediterranean plankton communities and carbon export under present and future conditions of pH and temperature. *Biogeosciences* 18, 5423–5446. doi: 10.5194/bg-18-5423-2021
- Giovagnetti, V., Brunet, C., Conversano, F., Tramontano, F., Obernosterer, I., Ridame, C., et al. (2013). Assessing the role of dust deposition on phytoplankton ecophysiology and succession in a low-nutrient low-chlorophyll ecosystem: a mesocosm experiment in the Mediterranean Sea. *Biogeosciences* 10, 2973–2991. doi: 10.5194/bg-10-2973-2013
- Goericke, R., and Fry, B. (1994). Variations of marine plankton $\delta^{13}\text{C}$ with latitude, temperature, and dissolved CO_2 in the world ocean. *Global Biogeochem. Cycles* 8, 85–90. doi: 10.1029/93gb03272
- Gogou, A., Sanchez-Vidal, A., Durrieu De Madron, X., Stavrakakis, S., Calafat, A. M., Stabholz, M., et al. (2014). Reprint of: Carbon flux to the deep in three open sites of the Southern European Seas (SES). *J. Mar. Syst.* 135, 170–179. doi: 10.1016/j.jmarsys.2014.04.012
- Gogou, A., and Stephanou, E. G. (2004). Marine organic geochemistry of the Eastern Mediterranean. *Mar. Chem.* 85, 1–25. doi: 10.1016/j.marchem.2003.08.005
- Guerreiro, C. V., Baumann, K.-H., Brummer, G.-J. A., Fischer, G., Korte, L. F., Merkel, U., et al. (2017). Coccolithophore fluxes in the open tropical North Atlantic: influence of thermocline depth, Amazon water, and Saharan dust. *Biogeosciences* 14, 4577–4599. doi: 10.5194/bg-14-4577-2017
- Guerreiro, C. V., Baumann, K.-H., Brummer, G.-J. A., Korte, L. F., Sá, C., and Stuetz, J.-B. W. (2019). Transatlantic gradients in calcifying phytoplankton (coccolithophore) fluxes. *Prog. Oceanogr.* 176, 102140. doi: 10.1016/j.pocean.2019.102140
- Guerreiro, C. V., Baumann, K.-H., Brummer, G.-J. A., Valente, A., Fischer, G., Ziveri, P., et al. (2021). Carbonate fluxes by coccolithophore species between NW Africa and the Caribbean: Implications for the biological carbon pump. *Limnol. Oceanogr.* 66, 3190–3208. doi: 10.1002/lno.11872
- Guerreiro, C. V., Ferreira, A., Cros, L., Stuetz, J.-B., Baker, A., Tracana, A., et al. (2023). Response of coccolithophore communities to oceanographic and atmospheric processes across the North-and Equatorial Atlantic. *Front. Mar. Sci.* 10. doi: 10.3389/fmars.2023.1119488

Generative AI statement

The author(s) declare that no Generative AI was used in the creation of this manuscript.

Publisher's note

All claims expressed in this article are solely those of the authors and do not necessarily represent those of their affiliated organizations, or those of the publisher, the editors and the reviewers. Any product that may be evaluated in this article, or claim that may be made by its manufacturer, is not guaranteed or endorsed by the publisher.

Supplementary material

The Supplementary Material for this article can be found online at: <https://www.frontiersin.org/articles/10.3389/fmars.2025.1537028/full#supplementary-material>

- Guerzoni, S., Chester, R., Dulac, F., Herut, B., Loye-Pilot, M.-D., Measures, C., et al. (1999). The role of atmospheric deposition in the biogeochemistry of the Mediterranean Sea. *Prog. In Oceanogr.* 44, 147–190. doi: 10.1016/S0079-6611(99)00024-5
- Guieu, C. (2002). Chemical characterization of the Saharan dust end-member: Some biogeochemical implications for the western Mediterranean Sea. *J. Geophys. Res.* 107, D15. doi: 10.1029/2001jd000582
- Guieu, C., Ridame, C., Pulido-Villena, E., Bressac, M., Desboeufs, K., and Dulac, F. (2014). Impact of dust deposition on carbon budget: a tentative assessment from a mesocosm approach. *Biogeosciences* 11, 5621–5635. doi: 10.5194/bg-11-5621-2014
- Hamonou, E., Chazette, P., Balis, D., Dulac, F., Schneider, X., Galani, E., et al. (1999). Characterization of the vertical structure of Saharan dust export to the Mediterranean basin. *J. Geophys. Res.: Atmos.* 104, 22257–22270. doi: 10.1029/1999jd900257
- Hedges, J. I., Keil, R. G., and Benner, R. (1997). What happens to terrestrial organic matter in the ocean? *Organ. geochem.* 27, 195–212. doi: 10.1016/S0146-6380(97)00066-1
- Herut, B., Krom, M. D., Pan, G., and Mortimer, R. (1999). Atmospheric input of nitrogen and phosphorus to the Southeast Mediterranean: Sources, fluxes, and possible impact. *Limnol. Oceanogr.* 44, 1683–1692. doi: 10.4319/lo.1999.44.7.1683
- Herut, B., Rahav, E., Tsagaraki, T. M., Giannakourou, A., Tsiola, A., Psarra, S., et al. (2016). The potential impact of Saharan dust and polluted aerosols on microbial populations in the east Mediterranean sea, an overview of a mesocosm experimental approach. *Front. Mar. Sci.* 3. doi: 10.3389/fmars.2016.00226
- Herut, B., Zohary, T., Krom, M., Mantoura, R. F. C., Pitta, P., Psarra, S., et al. (2005). Response of East Mediterranean surface water to Saharan dust: On-board microcosm experiment and field observations. *Deep Sea Res. Part II: Topical Stud. Oceanogr.* 52, 3024–3040. doi: 10.1016/j.dsr.2005.09.003
- Huffman, G. J., Bolvin, D. T., Nelkin, E. J., and Adler, R. F. (2016). *TRMM (TMPA) Precipitation L3 1 day 0.25 degree x 0.25 degree V7*. Ed. A. Savtchenko (Greenbelt, MD, USA: Goddard Earth Sciences Data and Information Services Center (GES DISC)). doi: 10.5067/TRMM/TMPA/DAY/7
- Ignatiades, L., Gotsis-Skretas, O., Pagou, K., and Krasakopoulou, E. (2009). Diversification of phytoplankton community structure and related parameters along a large-scale longitudinal east–west transect of the Mediterranean Sea. *J. Plankton Res.* 31, 411–428. doi: 10.1093/plankt/fbn124
- Israelevich, P., Ganor, E., Alpert, P., Kishcha, P., and Stupp, A. (2012). Predominant transport paths of Saharan dust over the Mediterranean Sea to Europe. *J. Geophys. Res.: Atmos.* 117, D02205. doi: 10.1029/2011JD016482
- JPL MUR MEASURES Project (2015). *GHRST Level 4 MUR Global Foundation Sea Surface Temperature Analysis. Ver. 4.1* (CA, USA: PO.DAAC). doi: 10.5067/GHGMRF4FJ04
- Knappertsbusch, M. (1993). Geographic distribution of living and Holocene coccolithophores in the Mediterranean Sea. *Mar. Micropaleontol.* 21, 219–247. doi: 10.1016/0377-8398(93)90016-Q
- Koren, I., Joseph, J. H., and Israelevich, P. (2003). Detection of dust plumes and their sources in northeastern Libya. *Can. J. Remote Sens.* 29, 792–796. doi: 10.5589/m03-036
- Krom, M. D., Groom, S., and Zohary, T. (2003). “The Eastern Mediterranean,” in *Biogeochemistry of Marine Systems*. Eds. K. D. Black and G. B. Shimmield (Blackwell, New York), 91–122.
- Krom, M. D., Herut, B., and Mantoura, R. F. C. (2004). Nutrient budget for the Eastern Mediterranean: Implications for phosphorus limitation. *Limnol. Oceanogr.* 49, 1582–1592. doi: 10.4319/lo.2004.49.5.1582
- Lavigne, H., Civitarese, G., Gačić, M., and D’Ortenzio, F. (2018). Impact of decadal reversals of the north Ionian circulation on phytoplankton phenology. *Biogeosciences* 15, 4431–4445. doi: 10.5194/bg-15-4431-2018
- Lee, C., Armstrong, R. A., Cochran, J. K., Engel, A., Fowler, S. W., Goutx, M., et al. (2009a). MedFlux: investigations of particle flux in the Twilight Zone. *Deep Sea Res. Part II: Topical Stud. Oceanogr.* 56, 1363–1368. doi: 10.1016/j.dsr.2008.12.003
- Lee, C., Peterson, M. L., Wakeham, S. G., Armstrong, R. A., Cochran, J. K., Miquel, J. C., et al. (2009b). Particulate organic matter and ballast fluxes measured using time-series and settling velocity sediment traps in the northwestern Mediterranean Sea. *Deep Sea Res. Part II: Topical Stud. Oceanogr.* 56, 1420–1436. doi: 10.1016/j.dsr.2008.11.029
- Louis, J., Gazeau, F., and Guieu, C. (2018). Atmospheric nutrients in seawater under current and high pCO₂ conditions after Saharan dust deposition: Results from three minicosm experiments. *Prog. Oceanogr.* 163, 40–49. doi: 10.1016/j.pocan.2017.10.011
- Louis, J., Pedrotti, M. L., Gazeau, F., and Guieu, C. (2017). Experimental evidence of formation of transparent exopolymer particles (TEP) and POC export provoked by dust addition under current and high pCO₂ conditions. *PLoS One* 12, e0171980. doi: 10.1371/journal.pone.0171980
- Malinverno, E. (2003). Coccolithophorid distribution in the Ionian Sea and its relationship to eastern Mediterranean circulation during late fall to early winter 1997. *J. Geophys. Res.* 108, 8115. doi: 10.1029/2002jc001346
- Malinverno, E., Maffioli, P., Corselli, C., and De Lange, G. J. (2014). Present-day fluxes of coccolithophores and diatoms in the pelagic Ionian Sea. *J. Mar. Syst.* 132, 13–27. doi: 10.1016/j.jmarsys.2013.12.009
- Malinverno, E., Triantaphyllou, M. V., Stavrakakis, S., Ziveri, P., and Lykousis, V. (2009). Seasonal and spatial variability of coccolithophore export production at the South-Western margin of Crete (Eastern Mediterranean). *Mar. Micropaleontol.* 71, 131–147. doi: 10.1016/j.marmicro.2009.02.002
- Marañón, E., Van Wambeke, F., Uitz, J., Boss, E. S., Dimier, C., Dinasquet, J., et al. (2021). Deep maxima of phytoplankton biomass, primary production and bacterial production in the Mediterranean Sea. *Biogeosciences* 18, 1749–1767. doi: 10.5194/bg-18-1749-2021
- Marty, J.-C., Chiavérini, J., Pizay, M.-D., and Avril, B. (2002). Seasonal and interannual dynamics of nutrients and phytoplankton pigments in the western Mediterranean Sea at the DYFAMED time-series station, (1991–1999). *Deep Sea Res. Part II: Topical Stud. Oceanogr.* 49, 1965–1985. doi: 10.1016/S0967-0645(02)00022-X
- McGregor, H. V., Dupont, L., Stuu, J.-B. W., and Kuhlmann, H. (2009). Vegetation change, goats, and religion: a 2000-year history of land use in southern Morocco. *Quater. Sci. Rev.* 28, 1434–1448. doi: 10.1016/j.quascirev.2009.02.012
- Moulin, C., Lambert, C. E., Dayan, U., Masson, V., Ramonet, M., Bousquet, P., et al. (1998). Satellite climatology of African dust transport in the Mediterranean atmosphere. *J. Geophys. Res.: Atmos.* 103, 13137–13144. doi: 10.1029/98jd00171
- NASA Goddard Space Flight Center (2022). *Moderate-resolution Imaging Spectroradiometer (MODIS) Aqua Global Mapped Chlorophyll (CHL) Data* (Greenbelt, MD, USA: Ocean Ecology Laboratory, Ocean Biology Processing Group). doi: 10.5067/AQUA/MODIS/L3M/CHL/2022
- Nieuwenhuize, J., Maas, Y. E. M., and Middelburg, J. J. (1994). Rapid analysis of organic carbon and nitrogen in particulate materials. *Mar. Chem.* 45, 217–224. doi: 10.1016/0304-4203(94)90005-1
- Pabortsava, K., Lampitt, R. S., Benson, J., Crowe, C., McLachlan, R., Le Moigne, F. A. C., et al. (2017). Carbon sequestration in the deep Atlantic enhanced by Saharan dust. *Nat. Geosci.* 10, 189–194. doi: 10.1038/ngeo2899
- Patara, L., Pinardi, N., Corselli, C., Malinverno, E., Tonani, M., Santoleri, R., et al. (2009). Particle fluxes in the deep Eastern Mediterranean basins: the role of ocean vertical velocities. *Biogeosciences* 6, 333–348. doi: 10.5194/bg-6-333-2009
- Pedrosa-Pàmies, R., Parinos, C., Sanchez-Vidal, A., Calafat, A., Canals, M., Velaoras, D., et al. (2021). Atmospheric and oceanographic forcing impact particle flux composition and carbon sequestration in the Eastern Mediterranean sea: A three-year time-series study in the deep Ierapetra basin. *Front. Earth Sci.* 8. doi: 10.3389/feart.2021.591948
- Pedrosa-Pàmies, R., Parinos, C., Sanchez-Vidal, A., Gogou, A., Calafat, A., Canals, M., et al. (2015). Composition and sources of sedimentary organic matter in the deep eastern Mediterranean Sea. *Biogeosciences* 12, 7379–7402. doi: 10.5194/bg-12-7379-2015
- Platnick, S., Hubanks, P., Meyer, K., and King, M. D. (2015). *MODIS Atmosphere L3 Daily Product (08_L3)* (Greenbelt, MD, USA: NASA MODIS Adaptive Processing System, Goddard Space Flight Center). doi: 10.5067/MODIS/MYD08_D3.061
- Ploug, H., Iversen, M. H., and Fischer, G. (2008). Ballast, sinking velocity, and apparent diffusivity within marine snow and zooplankton fecal pellets: Implications for substrate turnover by attached bacteria. *Limnol. Oceanogr.* 53, 1878–1886. doi: 10.4319/lo.2008.53.5.1878
- Poulos, S. E. (2023). Water masses of the Mediterranean sea and Black sea: an overview. *Water* 15, 3194. doi: 10.3390/w15183194
- Prospero, J. M., Ginoux, P., Torres, O., Nicholson, S. E., and Gill, T. E. (2002). Environmental characterization of global sources of atmospheric soil dust identified with the Nimbus 7 Total Ozone Mapping Spectrometer (TOMS) absorbing aerosol product. *Rev. Geophys.* 40, 1002. doi: 10.1029/2000rg000095
- Pulido-Villena, E., R  rolo, V., and Guieu, C. (2010). Transient fertilizing effect of dust in P-deficient LNLc surface ocean. *Geophys. Res. Lett.* 37, L01603. doi: 10.1029/2009gl041415
- Pulido-Villena, E., Wagener, T., and Guieu, C. (2008). Bacterial response to dust pulses in the western Mediterranean: Implications for carbon cycling in the oligotrophic ocean. *Global Biogeochem. Cycles* 22, GB1020. doi: 10.1029/2007gb003091
- Rampen, S. W., Abbas, B. A., Schouten, S., and Sinninghe Damste, J. S. (2010). A comprehensive study of sterols in marine diatoms (Bacillariophyta): Implications for their use as tracers for diatom productivity. *Limnol. Oceanogr.* 55, 91–105. doi: 10.4319/lo.2010.55.1.0091
- Rampen, S. W., Friedl, T., Rybalka, N., and Thiel, V. (2022). The Long chain Diol Index: A marine palaeotemperature proxy based on eustigmatophyte lipids that records the warmest seasons. *Proc. Natl. Acad. Sci.* 119, e2116812119. doi: 10.1073/pnas.2116812119
- Rampen, S. W., Willmott, V., Kim, J.-H., Uliana, E., Mollenhauer, G., Schefu  , E., et al. (2012). Long chain 1, 13-and 1, 15-diols as a potential proxy for palaeotemperature reconstruction. *Geochim. Cosmochim. Acta* 84, 204–216. doi: 10.1016/j.gca.2012.01.024
- Reich, T., Ben-Ezra, T., Belkin, N., Tsemel, A., Aharonovich, D., Roth-Rosenberg, D., et al. (2022). A year in the life of the Eastern Mediterranean: Monthly dynamics of phytoplankton and bacterioplankton in an ultra-oligotrophic sea. *Deep Sea Res. Part I: Oceanogr. Res. Papers* 182, 103720. doi: 10.1016/j.dsr.2022.103720
- Ridame, C., Dekaezemacker, J., Guieu, C., Bonnet, S., L’Helguen, S., and Malien, F. (2014). Contrasted Saharan dust events in LNLc environments: impact on nutrient dynamics and primary production. *Biogeosciences* 11, 4783–4800. doi: 10.5194/bg-11-4783-2014
- Ridame, C., Dinasquet, J., Hallstr  m, S., Bigeard, E., Riemann, L., Van Wambeke, F., et al. (2022). N₂ fixation in the Mediterranean Sea related to the composition of the diazotrophic community and impact of dust under present and future environmental conditions. *Biogeosciences* 19, 415–435. doi: 10.5194/bg-19-415-2022

- Ridame, C., and Guieu, C. (2002). Saharan input of phosphate to the oligotrophic water of the open western Mediterranean Sea. *Limnol. Oceanogr.* 47, 856–869. doi: 10.4319/lo.2002.47.3.0856
- Rolph, G., Stein, A., and Stunder, B. (2017). Real-time environmental applications and display sYstem: READY. *Environ. Model. Softw.* 95, 210–228. doi: 10.1016/j.envsoft.2017.06.025
- Rumolo, P., Barra, M., Gherardi, S., Marsella, E., and Sprovieri, M. (2011). Stable isotopes and C/N ratios in marine sediments as a tool for discriminating anthropogenic impact. *J. Environ. Monit.* 13, 3399. doi: 10.1039/c1em10568j
- Scheuvs, D., Schütz, L., Kandler, K., Ebert, M., and Weinbruch, S. (2013). Bulk composition of northern African dust and its source sediments — A compilation. *Earth-Sci. Rev.* 116, 170–194. doi: 10.1016/j.earscirev.2012.08.005
- Skampa, E., Triantaphyllou, M., Dimiza, M., Gogou, A., Malinverno, E., Stavrakakis, S., et al. (2020). Coccolithophore export in three deep-sea sites of the Aegean and Ionian Seas (Eastern Mediterranean): Biogeographical patterns and biogenic carbonate fluxes. *Deep Sea Res II Top Stud Oceanogr.* 171, 104690. doi: 10.1016/j.dsr2.2019.104690
- Siokou-Frangou, I., Christaki, U., Mazzocchi, M. G., Montresor, M., Ribera D'Alcalá, M., Vaqué, D., et al. (2010). Plankton in the open Mediterranean Sea: a review. *Biogeosciences* 7, 1543–1586. doi: 10.5194/bg-7-1543-2010
- Stavrakakis, S., Gogou, A., Krasakopoulou, E., Karageorgis, A. P., Kontoyiannis, H., Rousakis, G., et al. (2013). Downward fluxes of sinking particulate matter in the deep Ionian Sea (NESTOR site), eastern Mediterranean: seasonal and interannual variability. *Biogeosciences* 10, 7235–7254. doi: 10.5194/bg-10-7235-2013
- Stein, A. F., Draxler, R. R., Rolph, G. D., Stunder, B. J. B., Cohen, M. D., and Ngan, F. (2015). NOAA's HYSPLIT atmospheric transport and dispersion modeling system. *Bull. Am. Meteorol. Soc.* 96, 2059–2077. doi: 10.1175/bams-d-14-00110.1
- Still, C. J., and Powell, R. L. (2009). "Continental-Scale Distributions of Vegetation Stable Carbon Isotope Ratios," in *Isoscapes: understanding movement, pattern, and process on Earth through isotope mapping*. Eds. J. B. West, G. J. Bowen, T. E. Dawson and K. P. Tu (Springer, Dordrecht), 179–194.
- Tegen, I., Harrison, S. P., Kohfeld, K., Prentice, I. C., Coe, M., and Heimann, M. (2002). Impact of vegetation and preferential source areas on global dust aerosol: Results from a model study. *J. Geophys. Res.: Atmos.* 107, 4576. doi: 10.1029/2001jd000963
- Ternon, E., Guieu, C., Loÿe-Pilot, M. D., Leblond, N., Bosc, E., Gasser, B., et al. (2010). The impact of Saharan dust on the particulate export in the water column of the North Western Mediterranean Sea. *Biogeosciences* 7, 809–826. doi: 10.5194/bg-7-809-2010
- Van der Does, M., Korte, L. F., Munday, C. I., Brummer, G. J. A., and Stuut, J. B. W. (2016). Particle size traces modern Saharan dust transport and deposition across the equatorial North Atlantic. *Atmos Chem Phys.* 16, 13697–13710. doi: 10.5194/acp-16-13697-2016
- Van Der Jagt, H., Friese, C., Stuut, J.-B. W., Fischer, G., and Iversen, M. H. (2018). The ballasting effect of Saharan dust deposition on aggregate dynamics and carbon export: Aggregation, settling, and scavenging potential of marine snow. *Limnol. Oceanogr.* 63, 1386–1394. doi: 10.1002/lno.10779
- Varga, G., Újvári, G., and Kovács, J. (2014). Spatiotemporal patterns of Saharan dust outbreaks in the Mediterranean Basin. *Aeolian Res.* 15, 151–160. doi: 10.1016/j.aeolia.2014.06.005
- Varkitzi, I., Psarra, S., Assimakopoulou, G., Pavlidou, A., Krasakopoulou, E., Velaoras, D., et al. (2020). Phytoplankton dynamics and bloom formation in the oligotrophic Eastern Mediterranean: Field studies in the Aegean, Levantine and Ionian seas. *Deep Sea Res. Part II: Topical Stud. Oceanogr.* 171, 104662. doi: 10.1016/j.dsr2.2019.104662
- Volkman, J. K. (2016). "Sterols in Microalgae," in *The Physiology of Microalgae*. Eds. M. A. Borowitzka, J. Beardall and J. A. Raven (Springer International Publishing, Cham), 485–505.
- Volkman, J. K., Eglinton, G., Corner, E. D. S., and Forsberg, T. E. V. (1980). Long-chain alkenes and alkenones in the marine coccolithophorid *Emiliania huxleyi*. *Phytochemistry* 19, 2619–2622. doi: 10.1016/S0031-9422(00)83930-8